Pharm Res (2011) 28:1870–1883
DOI 10.1007/s11095-011-0415-8

RESEARCH ARTICLE

Enhanced Oral Bioavailability of Vinpocetine Through Mechanochemical Salt Formation: Physico-Chemical Characterization and *In Vivo* Studies

Dritan Hasa • Dario Voinovich • Beatrice Perissutti • Mario Grassi • Alois Bonifacio • Valter Sergo • Cinzia Cepek • Michele R. Chierotti • Roberto Gobetto • Stefano Dall'Acqua • Sergio Invernizzi

Received: 12 January 2011 / Accepted: 1 March 2011 / Published online: 19 March 2011

ABSTRACT

Purpose Enhancing oral bioavailability of vinpocetine by forming its amorphous citrate salt through a solvent-free mechanochemical process, in presence of micronised crospovidone and citric acid.

Methods The impact of formulation and process variables (amount of polymer and citric acid, and milling time) on vinpocetine solubilization kinetics from the coground was studied through an experimental design. The best performing samples were characterized by employing a multidisciplinary approach, involving Differential scanning calorimetry, X-ray diffraction, Raman imaging/spectroscopy, X-ray photoelectron spectroscopy, solid-state NMR spectroscopy, porosimetry and *in vivo* studies on rats to ascertain the salt formation, their solid-state characteristics and oral bioavailability in comparison to vinpocetine citrate salt (Oxopocetine®).

Results The analyses attested that the mechanochemical process is a viable way to produce in absence of solvents vinpocetine citrate salt in an amorphous state.

Conclusion From the *in vivo* studies on rats the obtained salt was four times more bioavailable than its physical mixture and bioequivalent to the commercial salt produced by conventional synthetic process implying the use of solvent.

KEY WORDS mechanochemical reaction/activation · oral absorption · physico-chemical characterization · solvent-free process · vinpocetine citrate

INTRODUCTION

Vinpocetine (VIN) is a vincamine derivative and presents a series of very interesting pharmacological properties in relation to cerebral circulation, acting on vascular resistance, particularly in the area of blood vessels (1). It has been shown to improve cerebral circulation and metabolism in the management of various types of cerebrovascular

D. Hasa • D. Voinovich (✉) • B. Perissutti (✉)
Department of Chemical and Pharmaceutical Sciences
University of Trieste
P. le Europa 1
34127 Trieste, Italy
e-mail: vojnovic@units.it

B. Perissutti
e-mail: bperissutti@units.it

M. Grassi • A. Bonifacio • V. Sergo
Department of Industrial Engineering and Information Technology
University of Trieste
via Valerio 10
34127 Trieste, Italy

C. Cepek
CNR-IOM, TASC National Laboratory
Area Science Park, S.S. 14, km 163.5 Basovizza
34149 Trieste, Italy

M. R. Chierotti • R. Gobetto
Department of Chemistry I.F.M., Laboratory of NMR Spectroscopy
University of Torino
Via P. Giuria 7
10125 Turin, Italy

S. Dall'Acqua
Department of Pharmaceutical Sciences
University of Padova
via F. Marzolo 5
35131 Padova, Italy

S. Invernizzi
Department of Life Sciences
University of Trieste
Via Giorgieri 10
34127 Trieste, Italy

circulatory disorders, e.g. cerebral infarction, cerebral hemorrhage residual and cerebral arteries cirrhosis (2), and for the treatment of cognitive disorders and related symptoms (3). However, as a consequence of its low aqueous solubility and wettability, and extensive metabolism during first pass, VIN suffers from poor oral bioavailability (~6.7%) (4,5). Hence, faced with its various pharmacological properties, its clinical use is greatly restricted, so there is a need to improve its poor aqueous solubility to increase its oral absorption.

With this purpose, several approaches have been attempted. The most common consisted in its complexation in cyclodextrins, in some cases with the help of a ternary component (6–9), because VIN chemical structure allows at least a portion of the molecule to be housed inside the cavity of the cyclodextrins (9). Other experiences were intended to counteract its poor solubility and wettability by means of hydrophilic carriers (2,10) or to take advantage of its lipophilic character (its partition coefficient is ranging about 3 (11)) by incorporation in self-emulsifying systems (12–14).

Recently, our group has successfully increased the oral absorption by cogrinding VIN with micronized crospovidone in a planetary mill using an optimized mechanochemical activation process (15). In that experience, the mechanical loading has caused particles' comminuting and disordering of lattice structure, so that the solid has gained an activated state more prone to dissolution (e.g. by forming nanocrystalline or amorphous phases).

In the present research, with the aim of facilitating VIN oral absorption, the formation of the VIN water-soluble citrate was investigated. The transformation of the parent drug in the salt form permits rapid absorption and unaltered or even increased pharmacological actions (16). If the chemical approach is classical, the procedure adopted to prepare the salt is original. In fact, in this experience VIN citrate was obtained by proton transfer through a solid-state reaction conducted with the aid of the mechanical energy. To go into more details, VIN was subjected to a mechanochemical treatment in the presence of citric acid as a reactant and crosslinked polymer (micronized crospovidone) as a processing aid. In this case, the mechanical energy and, in particular, the shearing forces resulting from the rolling of ball elements on the wall of the planetary mill bowl were used for the dry synthesis of VIN citrate. In fact, the so-called pharmaceutical "mechanocomposites" can be successfully prepared by mechanical treatment of mixtures of the solid reactants, with the advantage of a more convenient, cheaper and environmentally friendly process (17). Thus, such an approach represents a solvent-free green technology in alternative to patented synthesis (16) involving the use of solvents.

After the preparation of 27 ternary coground systems with different compositions and 3 milling times, the best products were extensively characterized in comparison to starting VIN to verify the *in vitro* dissolution enhancement, and to commercial VIN citrate salt, Oxopocetine®, to verify the physico-chemical correspondence and bioequivalence of our product.

MATERIALS AND METHODS

Materials

VIN was a kind gift from Linnea SA (Riazzino-Locarno, CH). Oxopocetine® (vinpocetine citrate-VIN citrate) was kindly donated by Covex SA (Madrid, Spain). Citric acid was provided by Sigma-Aldrich (Milano, Italy). Micronized crospovidone (PVP-CL) was purchased from BASF (Ludwigshafen, Germany). All other analytical-grade chemicals and solvents of HPLC grade, were provided by Carlo Erba (Milan, Italy).

Preparation of Coground Mixtures

Drug and citric acid were coground in different drug-to-citric acid weight ratios in the presence of crospovidone in several drug-to-polymer weight ratios according to the experimental plan (Table I) in a planetary mill Fritsch P5 (Pulverisette, Contardi Fritsch s.r.l., Milan, Italy). The planetary mill was equipped by 4 agate cylindrical grinding chambers (internal height H_v=2.6 cm, internal radius R_v= 3.2 cm, internal volume = 27.5 cm^3) adopting agate balls (diameter 2.2 cm) as grinding media.

Six gram batches, previously blended in the suitable proportions with a stainless steel spatula, were simultaneously coground. The following operative conditions were selected on the basis of a previously published *ad hoc* mathematical model (18): maximum velocity (10,000 rpm), bowl loading (6 g), number of grinding media (6 agate balls).

The grinding procedure was pursued for 3 milling times, according to the experimental plan below reported, stopping every 5 min to homogeneously mix the mass with a stainless steel spatula. Three factors, 2 formulation variables (drug-to-citric acid wt ratio, X_1, and drug-to-polymer wt ratio, X_2) and a process variable (milling time, X_3) were selected for investigation. Each factor was considered in different experimental levels, selected during preliminary trials: 2 levels for drug-to-citric acid weight ratio, X_1 (1:1.1, 1:0.55 corresponding to 1:2 and 1:1 molar ratio, respectively), 3 levels for drug-to-polymer weight ratio, X_2 (1:2, 1:4, 1:7), and 3 experimental levels for milling time, X_3 (15, 30, 60 min). The

Table I Experimental Plan and Observed Response Values

Run[a]	Independent variables			Observed response (mean± S.D.; $n=3$)
	X_1 (wt ratio)	X_2 (wt ratio)	X_3 (min)	Y^b (mg/L)
1	1:0.55	1:2	15	8.51 ± 0.06
2	1:0.55	1:4	15	10.55 ± 0.50
3	1:1.1	1:7	15	8.05 ± 0.66
4	1:1.1	1:2	30	15.73 ± 0.41
5	1:0.55	1:4	30	12.39 ± 0.79
6	1:0.55	1:7	30	12.43 ± 0.95
7	1:0.55	1:2	60	8.94 ± 0.16
8	1:1.1	1:4	60	6.30 ± 0.83
9	1:0.55	1:7	60	7.34 ± 0.54

X_1 drug-to-citric acid wt ratio
X_2 drug-to-polymer wt ratio
X_3 milling time (min)
[a] three replicated experiments
[b] Y mean amount of solubilized drug after 120 min of analysis in pH 7.4 buffer

effect of these variables on a coground characteristic (amount of VIN solubilized in 120 min, Y) was statistically evaluated. The experimental plan (shown in Table I) was designed using NEMRODW program (19), and the statistical analysis was performed by standard R package (20). To reduce systematic errors, experiments were completely randomized.

Preparation of Physical Mixtures

Physical mixtures (PM) were prepared in batches of 12 g by manually mixing drug, citric acid and polymer with a stainless steel spatula for the standardized time of 5 min. The component weight proportions were selected according to the experimental plan. Six grams were then used for cogrinding experiments (see previous paragraph), and the rest was for comparison purposes.

Differential Scanning Calorimetry (DSC)

Calorimetric analyses were conducted using a differential scanning calorimeter (Mod. TA 4000, equipped with a measuring cell DSC 20 Mettler) using the STAR^e software version 9.30. The calibration of the instrument was carried out with indium, zinc and lead for the temperature, and with indium for the measurement of the enthalpy. Samples containing about 2 mg of VIN were placed in pierced aluminum pans and heated at a scanning rate of 10°C/min from 30 to 250°C, under static air.

X-Ray Powder Diffraction Studies (XRD)

XRD technique was employed to study the solid state of the samples using a D500 (Siemens, Munich, Germany) diffractometer with Cu-Kα radiation (1.5418Å), monochromatized by a secondary flat graphite crystal. The current was 20 mA and the voltage 40 kV. The scanning angle ranged from 5 to 35° of 2θ, steps were of 0.05° of 2θ, and the counting time was of 5 s/step.

Raman Imaging/Spectroscopy

Raman spectra and images were acquired for coground composites, PM and pure components using an inVia Raman system (Renishaw plc, Wotton-under-Edge, UK), equipped with a 300 mW diode NIR laser emitting at 785 nm (Renishaw) and a ProScanTMII motorized stage (Prior, Cambridge, UK). The laser was focused on the sample (consisting of 300-mg tablets with flat surfaces, prepared from physical and coground mixtures having different drug-to-citric acid and drug-to-polymer weight ratios, and from pure components) by a 50X objective (0.75 N.A.). To ensure a better sampling for each tablet by taking into account local variations in composition, an area of 84×84 μm was mapped with a grid of 2.8 μm (corresponding to 900 spectra per map) for each sample, using the Streamline^{TM} fast imaging configuration and the WiRE 3.1 software (Renishaw), with an total collection time of 13 min/map. Raman maps were then preprocessed (cosmic rays removal and baseline correction) and analyzed with the HyperSpec software package (21) for R (20), an average spectrum was calculated for each map, and images depicting the intensity ratio between VIN 1,610 cm^{-1} band and the PVP-CL 1,668 cm^{-1} band were produced.

X-Ray Photoelectron Spectroscopy (XPS)

All XPS spectra were acquired at room temperature in normal emission geometry using a conventional Mg K_α X-ray source (hv=1253.6 eV) and a 120° hemispherical electron energy analyser (overall energy resolution: about 0.8 eV). The binding energy scale has been calibrated by fixing the C 1*s* photoemission line due to hydrocarbon to 284.6 eV. All spectra were normalized to the incident

photon flux and were analysed by performing a non-linear mean square fit of the data following the Levenberg-Marquardt algorithm. A linear background was used, and the total photoemission intensity was reproduced by using Gaussian profiles.

Solid-State Nuclear Magnetic Resonance (SS NMR) Spectroscopy

^{15}N SS NMR spectra were recorded on a Bruker Avance II 400 instrument operating at 400.23 and 40.55 MHz for ^{1}H and ^{15}N nuclei, respectively. Cylindrical 4 mm o.d. zirconia rotors with a sample volume of 120 μL were employed and spun at 7 kHz. A ramp cross-polarization pulse sequence was used with a contact time of 4 ms, a ^{1}H 90° pulse of 3.05 μs, recycle delays of 3–15 s, and 15,000–26,000 transients. A two pulse phase modulation (TPPM) decoupling scheme was used with an rf field of 75 kHz. ^{15}N chemical shifts were referenced with the resonance of $(NH_4)_2SO_4$ (^{15}N signal at $\delta = 355.8$ ppm with respect to CH_3NO_2).

Porosity Measurements

The porosity of the samples was determined by a mercury porosimeter (ThermoQuest) equipped by Macropore Pascal 140 low pressure porosimeter and Macropore Pascal 240 high pressure porosimeter (CE Instruments, Italy). A dilatometer for powders with capillary diameter of 1.5 mm was loaded with 300 mg samples. Before measuring, a degasification procedure under vacuum pressure for 30 min was performed. The experiments were performed in triplicate. The size distribution was calculated applying the Mayer and Stowe method (22).

Dissolution Kinetics Tests (DKT)

Release tests, performed in triplicate, were led in 150 cm^3 of 0.2 M KH_2P0_4/0.2 M NaOH (pH 7.4) at 37±0.3°C. At this pH value the estimated solubility of pure VIN was 1.6 mg/l. At time zero, a suitable amount of sample (as a pure compound or ternary systems) to give 5 mg of active was added to the release environment. Uniformity conditions were ensured by using an impeller (rotational speed 200 rpm). The use of a fiber optic apparatus (HELLMA, Milano, Italy), connected to a spectrophotometer (ZEISS, Germany, wavelength 270.19 nm), permitted the determination of VIN concentration without perturbing the release environment (each release test lasted 120 min). Moreover, this methodology, previously successfully employed for coground systems containing VIN (15), allowed for easily overcoming the problem connected to drug concentration measurements in the presence of a dispersion of solid particles. Indeed, whilst the maximum VIN absorption occurred at 270.19 nm, the maximum citric acid absorption was at 220.49 nm, and the scattering effect due to polymeric particles uniformly occurred at every wavelength. Accordingly, the real absorbance associated to VIN concentration was the difference between the absorbance measured at 270.19 nm and that measured at 500.49 nm (at 500.49 nm VIN did not absorb). Non-sink conditions were used in release environment.

In Vivo Absorption Studies

Procedures for rats' care and management complied with those required by Italian laws (D.L.vo 116/92) and associated guidelines in the European Communities Council Directive of 24 November 1986 (86/609 ECC). Further, they adhered to ethical standards for humane treatment of experimental animals established by the ethical committee of University of Trieste.

Sprague-Dawley rats (450 g weight) were supplied by Centro Servizi Polivalenti di Ateneo (University of Trieste). Rats, with free access to water, were fasted overnight. Each experimental formulation was administered to 4 rats by gastric gavage in the form of aqueous suspensions (2 ml corresponding to a dose 11 mg/kg of VIN).

Blood samples (600 μl) were then collected using the "cannulated" tail artery method (23) in heparinized tubes at 30, 60, 90, 120, 180 and 360 min after administration. Blood samples were added of 66 μl of a 40 mM tetrasodium EDTA solution, centrifuged at 166 g for 10 min, and plasma was separated, immediately frozen at −80°C, and stored at this temperature until the analysis.

Assays of Vinpocetine in Powder and Plasma Samples

HPLC Analysis

For the determination of the drug content in the PM, coground systems and pure compounds, the procedure was the following: a suitable amount of powdered sample was accurately weighed and transferred to a 100 ml volumetric flask and diluted with acetonitrile. The mixture was subjected to sonication for 10 min and then filtered through a syringe filter (RC 0.45 μm, Phenomenex, Castel Maggiore, Bologna) to remove any particles. The first 5 μl of the filtrates were discarded, while the subsequent was collected. Then, an appropriate amount of the filtrate was diluted with acetonitrile and assayed by a validated high pressure liquid chromatographic (HPLC) with mass spectrometry (MS) detection method (24) already used in our previous work (15).

As for the determination of VIN in plasma samples, the following procedure was adopted: 600 µl methanol were added to 200 µl plasma, and the resulting mixture was vortexed for 10 min. After centrifugation (1,845 g for 6 min), 5 µl of the solution was injected. The VIN determination was carried out using the aforementioned method.

PHARMACOKINETIC ANALYSIS

Pharmacokinetic parameters were calculated on the plasma curves. The area under the plasma concentration-time curve, extrapolated to the last sampling time at which a quantifiable concentration is found ($AUC_{t=6}$), was calculated using the log-linear trapezoidal method. Time and value of maximum concentration (t_{max} and C_{max}, respectively) were reported as observed. The relative bioavailability of after oral administration (F_{rel}) was calculated in Eq. 1:

$$F_{rel} = \frac{AUC_{(\text{Coground or Commercial salt})}}{AUC_{(PM)}} \quad (1)$$

Pharmacokinetic analysis was carry out using WinNonlin Version 5.2 (Pharsight Corporation, Mountain View, CA) software.

AGING STUDIES

The best performing sample was kept at 25°C in a thermostated oven and subjected to DSC and XRD analyses every 9 months over a period of 18 months.

RESULTS AND DISCUSSION

The aim of the work was to enhance the solubility of VIN, and thereby improve its oral bioavailability, by means of water-soluble citrate salt formation. After the preparation, the best samples were extensively characterized in comparison to starting VIN to verify the *in vitro* dissolution enhancement, and in comparison to commercial VIN citrate salt, Oxopocetine®, to verify the physico-chemical correspondence and bioequivalence of our product.

In particular, to prepare the salt as an alternative to patented procedure of VIN citrate involving the use of solvents (16), a solid-state reaction conducted with the aid of the mechanical energy was used, employing micronized crospovidone as a processing aid and citric acid as a reactant.

This hydroxyacid, commonly used in pharmaceutical preparations, is frequently employed as dissolution enhancer in ternary mixtures (25) and has the property to form amorphous structures with poorly soluble drugs when processed in certain conditions (26). Further, it possesses favorable physical properties for an use in solid-solid reactions, such as its glass transition in the dry state of 11°C (26). In fact, it must be borne in mind that the plasticity of the reactants is a factor of primary importance in solid-solid reactions, since it influences the ease with which the contacts between the reactants are formed (17).

Micronized crospovidone, whose compatibility with VIN has been previously demonstrated (15), in earlier mechanochemical experiences has shown its ability to reduce drug adhesion to the grinding media and to the walls of the mixing bowl (27). Moreover, the amorphous polymer network can act as a stabilizer towards the drug metastable activated status possibly resulting from high energy milling (17,28). In addition, the presence of a certain amount of water in the polymer (29) may decrease the fragility of the citric acid (26), favoring its solid reactivity. Finally, the polymer can positively contribute to the active dissolution performance by preventing one of the major concerns about pharmaceutical salts of poorly water-soluble weak bases, e.g. the precipitation of the salt at pH values found in the g.i. tract (30).

The grinding process was conducted in optimized conditions using a Fritsch P5 planetary mill that is particularly suitable for its lab scale for performing a study of screening among variables. In this apparatus the mechanocomposite is mainly obtained by the creation of shearing interactions, as a result of the rolling of ball elements on the wall of the grinding container.

The grinding procedure was carried out using different sample compositions and three operating conditions according to the experimental plan reported in Table I. In particular, three factors, two formulation variables (drug-to-citric acid wt ratio, X_1, and drug-to-polymer wt ratio, X_2), and a process variable (milling time, X_3) were selected for investigation. Each factor was considered in different experimental levels, selected during preliminary trials: two levels for drug-to-citric acid weight ratio (X_1), three levels for drug-to-polymer weight ratio (X_2) and three experimental levels for milling time (X_3). The effect of these variables was statistically evaluated on the amount of solubilized drug after 120 min from the coground product (Y), in consideration of the aim of the research. To reduce systematic errors, the resulting 27 experiments were run randomly.

An inspection of the boxplots (Fig. 1) suggested that a remarkable influence of the response was only obtained from the milling time variable (X_3) where 30 min factor level showed a significant improvement of the output Y.

However, for a better statistical evaluation, so-called Tukey's "Honest Significant Difference" (HSD) 95% method data was computed. To compare the means of

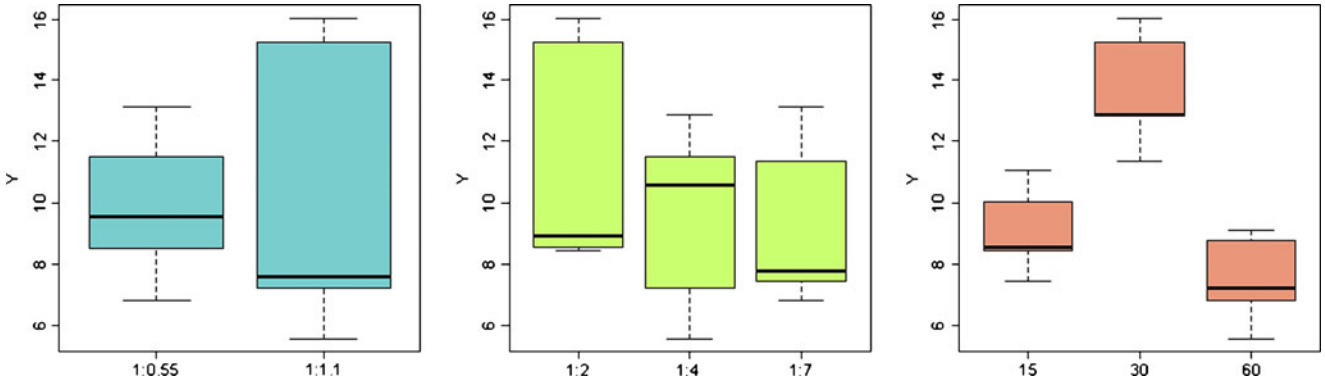

Fig. 1 Raw data boxplots corresponding to measures Y *vs.* factors X_1, X_2, X_3 of experimental design on Table I. The thick line represents the median for each boxplot.

output Y (the amount of drug solubilized after 120 min), the levels of factors X_1, X_2 and X_3 have been ordered according to increasing mean of Y, before taking differences, so that the calculated differences in the means are positive. The results are listed in Table II and represented in a graph-mode in Fig. 2.

From these data, the influence of VIN-citric acid weight ratio (X_1) on the drug dissolution was not significant ($p=0.948$).

Conversely, very interesting was the effect of the drug-to-polymer weight ratio (X_2): the lower the amount of polymer used, the higher the amount of solubilized drug, probably because a large amount of polymer reduces the possibility of interaction between citric acid and VIN. The number of contacts between reacting particles is in fact of crucial importance for solid-solid reactions (17). It was emphasized that sometimes, for the rate of interaction, the formation of contacts is a limiting step more important than the rate of the chemical reaction itself (17).

The time factor (X_3) was the most influencing parameter, and 30 min is the optimal processing time. It appeared that an activation time of 15 min is not sufficient to achieve the maximum concentration of VIN in solution. On the contrary, the mechanical energy given in 60 min was excessive and induced a worsening of the performance. One possibility is that milling contributes to hydrophobicity because of air adsorption to the new formed surfaces. A further possible explanation of the deterioration of the solubilization performances with increased milling time may be an increased particle size of the coground system (from 30 to 60 min of milling time). This hypothesis was verified by analyzing the particle size of a coground system (1:1.1:2 drug-to-citric-acid-to-polymer wt ratio) after 30 and 60 min of milling process. In Fig. 3 the differential distribution as a function of the diameter in a log scale is depicted. Both samples showed a monomodal distribution, with a peak frequency value of 23.6 μm in the case of 30 min coground and of 44.9 μm for 60 min coground. This data attested that continued milling time did not reduce particle size further; rather, the particle size raised remarkably. Probably crospovidone, necessary for avoiding adhesion phenomena to the grinding elements, was responsible for the undesired formation of agglomerates with the longest milling times, as in previous mechanochemical experiences (27,31). Large agglomerates are undesired not only from the dissolution point of view but also in considerations of their influence on the development of the mechanically activated solid-state reaction. In fact, it is well known that the correct adjustment of the size distribution of the particles in the reaction mixture in such a way as to provide the densest packing and prevent aggregation is important (32).

From the screening analysis it can be deduced that the best activation results are expected from the ternary systems containing a low amount of PVP-CL, processed for an intermediate time (30 min). As for citric acid content (X_1), the dissolution performances of the systems having different drug-to-citric acid wt ratios were not significantly different; hence, both ratios were selected for supplementary analyses. Therefore, the systems selected for further considerations were the following: 1:1.1:2 drug-to-citric-acid-to-polymer wt ratio coground for

Table II Differences, and Related Significance Between Observed Responses Associated to Each Level (See Table I) of the Three Considered Factors

Factor	Level difference	Mean difference	Significance
X_1	1:0.55–1:1.1	0.034	0.948
X_2	1:4–1:7	0.582	0.603
	1:2–1:7	1.880	0.013*
	1:2–1:4	1.298	0.101
X_3	15–60	1.526	0.047*
	30–60	6.040	0.000**
	30–15	4.514	0.000**

Significance codes (α): *$p=0.05$, **$p=0.001$

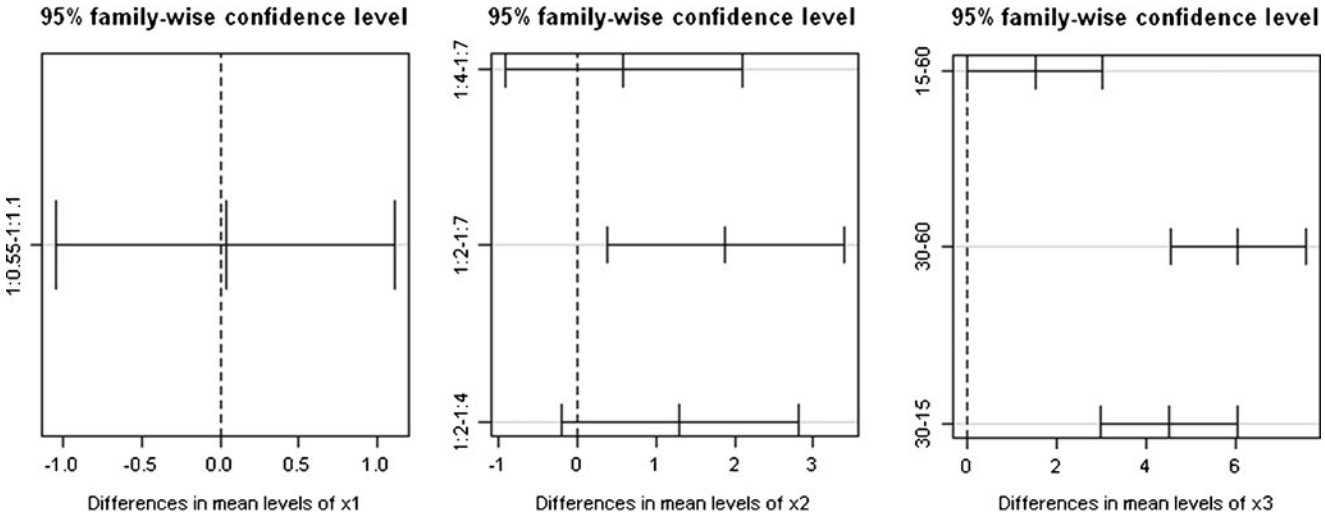

Fig. 2 Tukey's Significant Difference (HSD) 95% confidence intervals for the three considered variables influencing the response Y. Factor levels have been ordered. The significant differences at level (α) = 0.05 are those for which the left end point of the plotted interval is positive.

30 min and 1:0.55:2 drug-to-citric-acid-to-polymer wt ratio for 30 min. For the sake of brevity, these samples are named 1:1.1:2 and 1:0.55:2, respectively.

Figure 4 shows a great improvement of the solubilization kinetics, in terms of rate and extent of dissolved drug, in comparison to the pure VIN and the simple PM of the three components. To go into more details, in the DKT of the coground, the presence of a very rapid onset in the first 15 min of analysis followed by a pronounced supersaturation phenomenon was observed. An analogous initial burst phenomenon was noticed in the DKT of the commercial salt (also reported in Fig. 4). In the second part of the dissolution process the coground was able to maintain higher levels of solubilized VIN, thanks to the presence of the polymer, because the PVP-CL has the property of reducing in solution crystallization phenomena of poorly soluble drugs, as demonstrated by a recent study (33).

In the subsequent step, the solid state characterization of the coground samples was performed in comparison to pure components, ternary PM and the reference salt to study the influence of the mechanical treatment on the physical state of the drug.

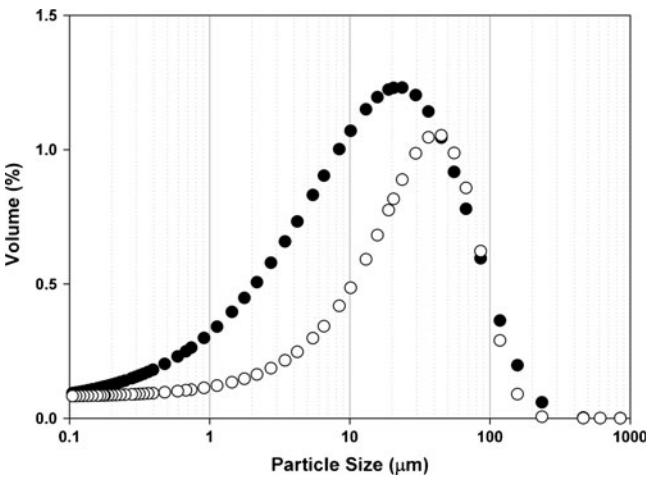

Fig. 3 Differential distribution of 1:1.1:2 drug-to-citric acid-to polymer wt ratio coground for 30 min (●) and 60 min (○) as a function of the diameter in a log scale.

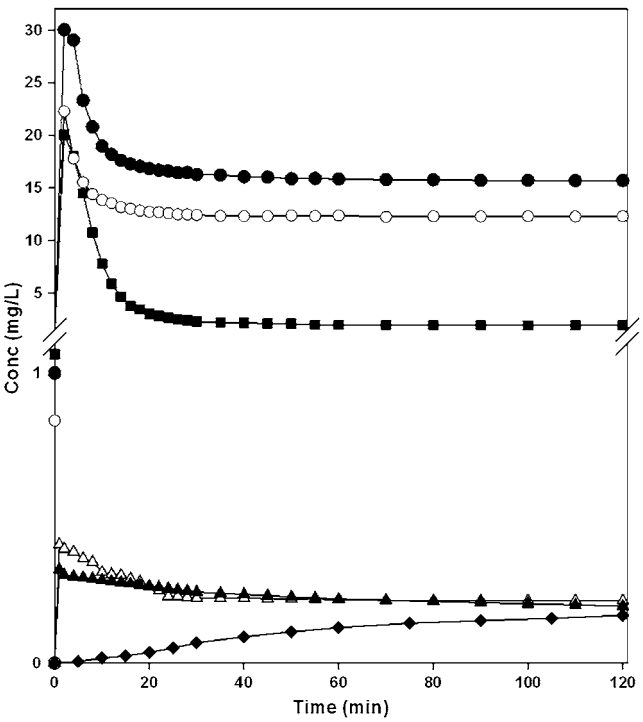

Fig. 4 *In vitro* solubilization kinetics in pH 7.4 of the ternary coground 1:1.1:2 (●), 1:0.55:2 after 30 min of milling (○), VIN salt (Oxopocetine®) (■), 1:1.1:2 PM (Δ), 1:0.55:2 PM (▲) and pure VIN (♦).

First, the ternary 1:1.1:2 and 1:0.55:2 coground systems were subjected to XRD analysis. In the pattern of PVP-CL (Fig. 5a), a complete lack of peaks and a halo pattern, typical of amorphous materials, was detected. Conversely, the crystalline drug showed intense reflections in the range between 10 and 25° of 2θ (Fig. 5b), in accordance to those previously reported for VIN by Ribeiro *et al.* (7) and Hasa *et al.* (15). The peaks of the citric acid (Fig. 5c) were detected in all the range of analysis, but in particular those at 14.1, 18, 25.8, 28.8 and 32.3° of 2θ were worth noticing because they can permit an easy distinction from VIN in multicomponent mixtures. Ternary PM patterns (Fig. 5d and f) are simply the sum of the reflections of the drug and the citric acid, without any sign of interaction. In the 1:0.55:2 coground system (Fig. 5e), the diffractogram showed the presence of residual peaks attributable to both VIN and citric acid. This suggested only a partial amorphysation of components. The situation is completely different in the case of 1:1.1:2 coground system where a modest hump due to the attenuation of citric acid signals between 5 and 12° of 2θ was visible, together with two peaks at 26.3 and 32.4° of 2θ attributable to residual-free (un-reacted) citric acid.

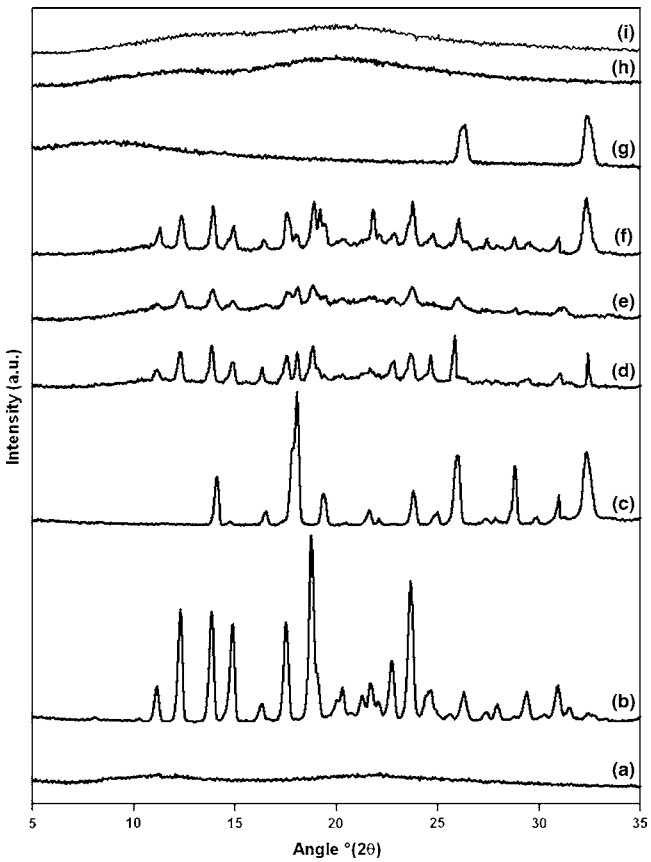

Fig. 5 PXRD Patterns: PVP-CL (**a**), pure VIN (**b**), pure citric acid (**c**), 1:0.55:2 PM (**d**), 1:0.55:2 coground system (**e**), 1:1.1:2 PM (**f**), 1:1.1:2 coground system (**g**), Oxopocetine® (**h**) and 1:1.1:2 coground system 18 months after preparation (**i**).

Finally, Oxopocetine® appeared completely amorphous at the XRD analysis (Fig. 5h). Its baseline was dominated by two humps between 5 and 25° of 2θ, in correspondence to original VIN and citric acid signals, here attenuated.

The physical characterization was pursued by means of DSC analysis. Pure VIN (Fig. 6b) exhibited a solid–liquid transition at 149.6°C, while citric acid presented an endothermal event at 156.7°C due to its melting, immediately followed by its degradation in air atmosphere (Fig. 6c). Crospovidone (Fig. 6a) in the considered temperature range lost its water between 30 and 120°C, starting its slow degradation at about 185°C. The DSC curve of the PM testified the absence of interactions among components (Fig. 6d and f). Conversely, in the 1:0.55:2 coground (Fig. 6e), according to previous XRD findings, a weak thermal event at about 145°C suggested the presence of nanocrystalline structures. For the 1:1.1:2 coground (Fig. 6g) no significant events of melting (attributable to the drug or to the citric acid) were visible; this means that neither of the two original crystalline components was still detectable in this sample. Unlike from the previous XRD analyses, in the DSC curve of this coground, no thermal event attributable to the components was detected. The commercial salt (Fig. 6h) did not show event of melting, but only a peak around 60°C and a moderate hump ranging about 170°C. The first thermal event is probably attributable to monohydrate citric acid, which, according to literature, shows in this range of temperatures its melting accompanied by the release of crystal water (34). As for the endothermal event at about 170°C, it is reported that citric acid when heated above 175°C is converted in decomposition substances by elimination of water and other components (35).

Further information was gathered from Raman imaging/spectroscopy. First, the effect of the co-grinding process on the spatial heterogeneity of the mixtures at microscopic level was evaluated. Comparison of Raman images of the 1:1.1:2 PM and coground (Fig. 7 left and right, respectively) revealed pronounced differences: an inhomogeneous distribution of VIN could be seen in the intensity Raman map of the PM (left), whereas a more homogeneous VIN distribution was observed in the Raman map of the 1:1.1:2 coground sample (right).

Raman spectra of PM (Fig. 8d and f) were a superimposition of the spectra of pure VIN and PVP-CL, whereas no bands due to citric acid (Fig. 8b) were detected. The absence of citric acid bands could be due to its smaller Raman cross-section with respect to the other two components. In both PM spectra, frequencies and relative intensities of the bands due to VIN were unaffected with respect to the spectrum of pure VIN (Fig. 8c), indicating the absence of any interaction between VIN and the other components. This observation is in agreement with our

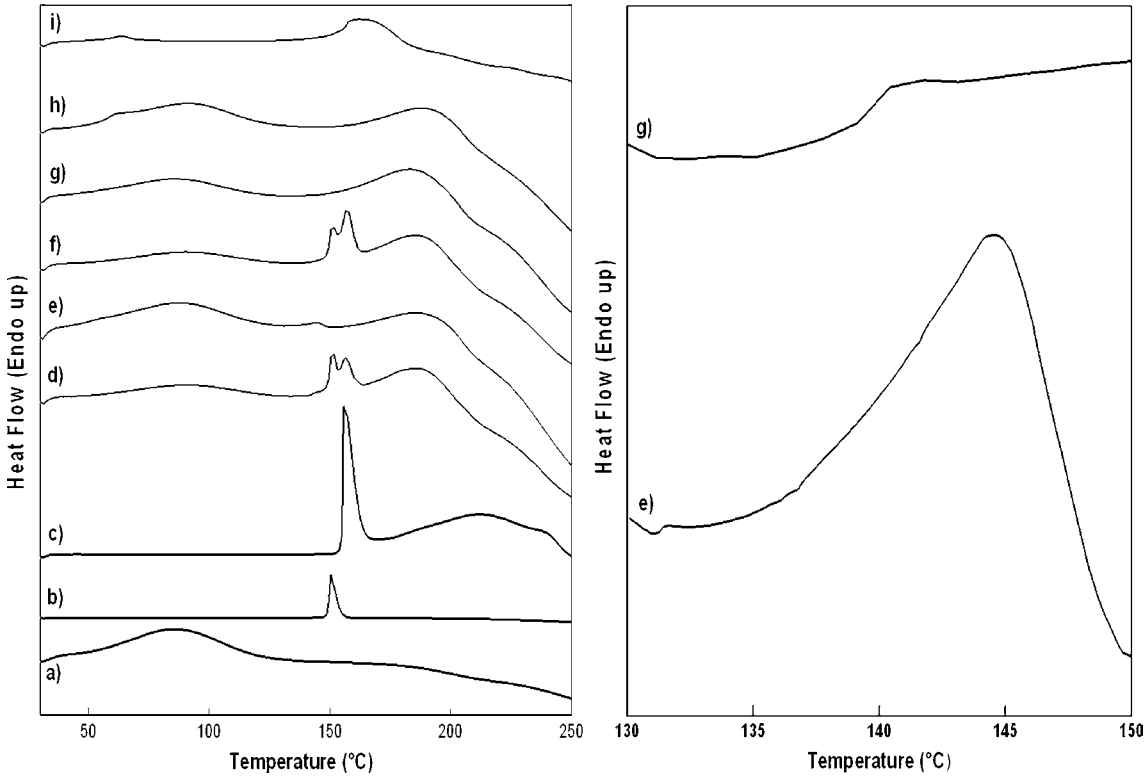

Fig. 6 Left: DSC traces of PVP-CL (**a**), pure VIN (**b**), pure citric acid (**c**), 1:0.55:2 PM (**d**), 1:0.55:2 coground system (**e**), 1:1.1:2 PM (**f**), 1:1.1:2 coground system (**g**), 1:1.1:2 coground system 18 months after preparation (**h**), and Oxopocetine® (**i**). Right: a particular of the 130–150°C temperature range in the DSC curve of 1:0.55:2 coground system (**e**) and 1:1.1:2 coground system (**g**).

recent Raman data on binary mixtures of VIN and PVP-CL (15). The situation was different in the case of the coground samples (Fig. 8e and g), whose Raman spectra cannot be reconstructed by a simple superposition of the pure components. In these spectra, the intense band due to an aromatic C=C stretching in VIN, which was found at 1,610 cm^{-1} in spectra of pure VIN and in PM, was split into a doublet, with the second band broader than the first at 1,622 cm^{-1}. The same changes occured for the C=O stretching band observed at 1,716 cm^{-1} in pure VIN, which in the coground Raman spectra underwent a broadening and a shift to 1,728 cm^{-1}. Such spectral changes, which were significantly more pronounced in the 1:1.1:2 than in the 1:0.55:2 coground sample, were to be

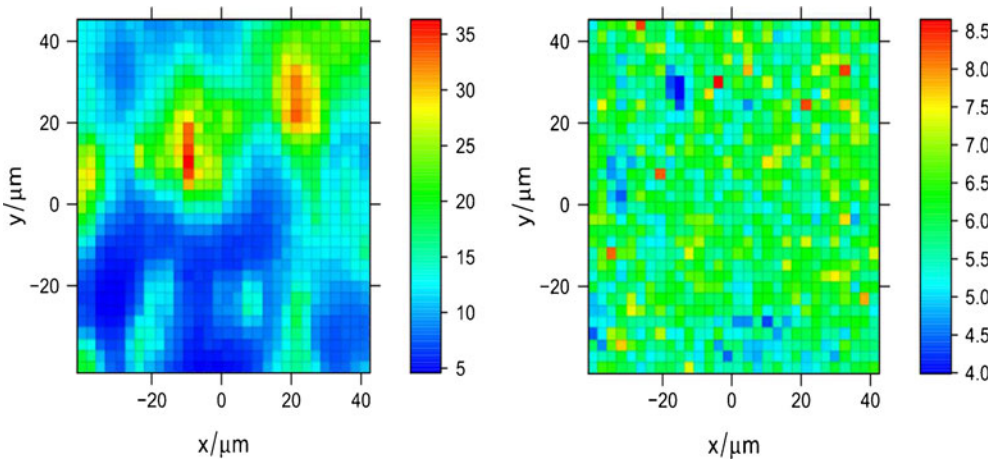

Fig. 7 Images depicting the density distribution of VIN in tablets consisting of PM (left) and coground system (right) of VIN, citric acid and PVP-CL in a 1:1.1:2 weight ratio. Images are constructed from Raman maps upon imaging the intensity ratio between the C=C stretching band of VIN (at 1,610 cm^{-1} for PM and at 1,622 cm^{-1} for coground system) and the 1,668 cm^{-1} band (C=O stretching) of PVP-CL.

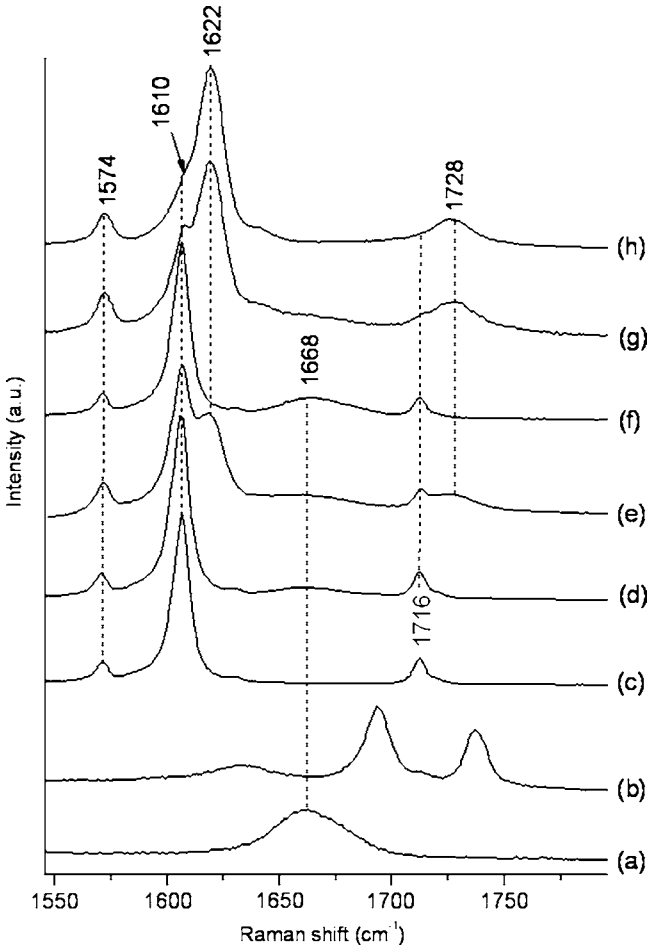

Fig. 8 1,550–1,800 cm^{-1} regions of Raman spectra of tablets of PVP-CL (**a**), citric acid (**b**), pure VIN (**c**), PM 1:0.55:2 (**d**), 1:0.55:2 coground system (**e**), PM 1:1.1:2 (**f**), 1:1.1:2 coground system (**g**) and Oxopocetin® (**h**); (**d**)–(**h**) are averages obtained from Raman maps of 84 × 84 μm containing 900 spectra each. Excitation wavelength is 785 nm.

interpreted as an alteration of the VIN C=C and C=O enviroments in the coground samples with respect to the pure substance. Interestingly, similar spectral changes, although less pronounced, have been observed for binary coground mixtures of VIN and PVP-CL (15) and can be interpreted as the disruption of the drug crystals. The larger band shift, with respect to pure VIN, observed in the 1:1.1:2 coground in comparison to 1:0.55:2 coground (Fig. 8g and e, respectively), clearly indicated an important role of citric acid in the disruption of VIN crystalline form. The Raman spectrum of the 1:1.1:2 composite sample, in which the changes with respect to pure VIN were more pronounced, was remarkably similar to that of Oxopocetin®, implying that VIN had the same form in both preparations.

From the aforementioned analyses, the formation of a readily soluble amorphous solid can be concluded, probably due to the formation of the amorphous citrate salt of VIN. To ascertain this point, additional investigations were conducted, taking as a reference the commercial salt (Oxopocetine®). In particular, X-ray photoelectron spectroscopy (XPS) and ^{15}N cross-polarization magic angle spinning (CPMAS) SS NMR experiments were selected because they are reported to be ideally suited for establishing the location of the proton in amorphous systems (36).

Figure 9 compares the N 1*s* XPS spectra (dots) of pure VIN (a), the polymer (b), the 1:1.1:2 coground system (c) and the VIN citrate commercial salt (Oxopocetine®) (d). Due to different charging shifts observed in all the measured samples, the binding energy scale was calibrated by fixing the C 1*s* photoemission line due to hydrocarbon to 284.6 eV (spectra not shown). The N 1*s* spectrum of pure VIN shows two components, corresponding to the two inequivalent nitrogen atoms present on the molecule, N1 and N4 (Fig. 9a). The binding energies 400.3 eV and 398.9 eV are attributable to VIN N1 and N4, respectively. The N 1*s* XPS level of the polymer has an intermediate energy and shows an intense and broad peak centered at 399.1 eV (Fig. 9b). Even though this peak was significantly broader than the others (1.8 eV *vs* 1.4), the data were reproduced by using only one component, because of sample inhomogeneity and disorder. The N 1*s* spectrum of the VIN citrate commercial salt (Oxopocetine®) (Fig. 9c) showed two main peak components at 400.4 eV and 401.4 eV. The peak at lower binding energy corresponded, within the experimental error, to N1 atoms of pure VIN, and the highest binding energy peak to the N4 nitrogen atoms after protonation. Taking into account the previous results and the spectrum lineshape, the N 1*s* spectrum of the 1:1.1:2 coground system (Fig. 9c) was reproduced using three peak components, which were found to be at 399.2 eV, 400.2 eV and 401.5 eV. The component at 399.2 eV corresponds to the polymer, while the component at 400.2 eV corresponds to N1 atoms. Finally, the peak at the highest binding energy (401.5 eV) was attributed to the N4 protonation by comparing this spectrum with that of Oxopocetine®. These results indicated the formation of VIN citrate by proton transfer through a solid-state reaction conducted with the aid of the mechanical energy.

In the case of SS NMR, it is possible to evaluate the protonation state of amino and carboxylic groups either from their isotropic chemical shifts or from the chemical shift anisotropy (37). The ^{15}N chemical shift is a useful parameter for the location of the hydrogen in hydrogen bonded systems involving nitrogen and oxygen atoms. Indeed, the ^{15}N chemical shift is more sensitive to protonation or to the presence of hydrogen bonds than that of other nuclei, such as ^{1}H and ^{13}C, due to its wider chemical shift range. Protonations as well as intermolecular hydrogen bonds produce high- or low-frequency shifts in the ^{15}N values, according to the type of nitrogen atom and to the type of interaction (38).

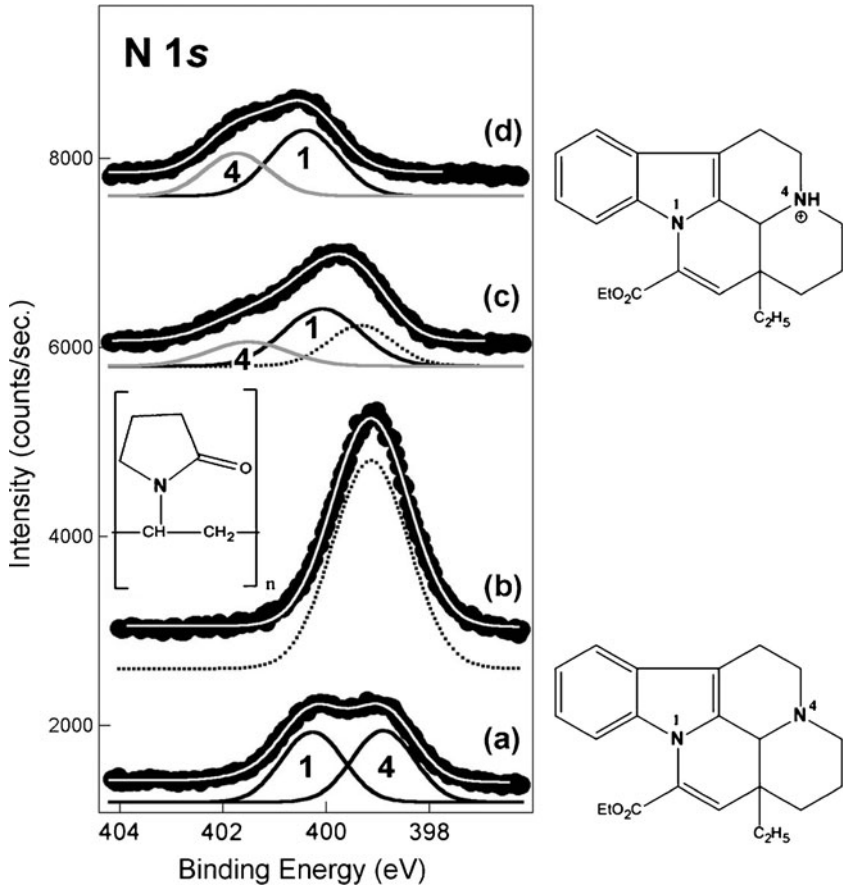

Fig. 9 XPS N 1s spectra of (**a**) pure VIN, (**b**) PVP-CL, (**c**) 1:1.1:2 coground system, and (**d**) Oxopocetine®. All spectra are normalized to the incident photon flux and have been analysed by performing a non-linear mean square fit of the data following the Levenberg-Marquardt algorithm. A linear background was used, and the total photoemission intensity (*white line*) was produced by using Gaussian profiles (*dotted line*).

Figure 10 shows the ^{15}N CPMAS spectra of VIN, PVP-CL, Oxopocetine®, and of the coground sample.

The VIN spectrum was characterized by two resonances at 4.0 and 113.6 ppm for N4 and N1, respectively. Pyrrolidone nitrogen atoms of the polymer gave rise to a broad (width at half height = 480 Hz) signal around 104.6 ppm in agreement with the high heterogeneity of a polymeric system (Fig. 10b). In the Oxopocetine® spectrum, no significant variations were observed in the N1 chemical shift (111.3 ppm) with respect to that of VIN. On the other hand, the N4 resonance was shifted to 19.0 ppm, clearly indicating a protonation of the group. The spectrum of the coground sample presented a broad signal (width at half height = 560 Hz) at about 108.7 ppm and a peak at 18.8 ppm. The former was attributed to the polymer nitrogen atoms with overlapped components around 144 ppm due to VIN N1 atoms. The latter was assigned to VIN N4 atoms, indicating that in the coground sample the VIN molecules were protonated as well as in the Oxopocetine®.

Hence, it can be concluded that the combination of the analytical techniques demonstrates the formation of the citrate salt of VIN in an amorphous solid form. This is in agreement to previous literature data (26) reporting that citric acid has the tendency to form amorphous structures.

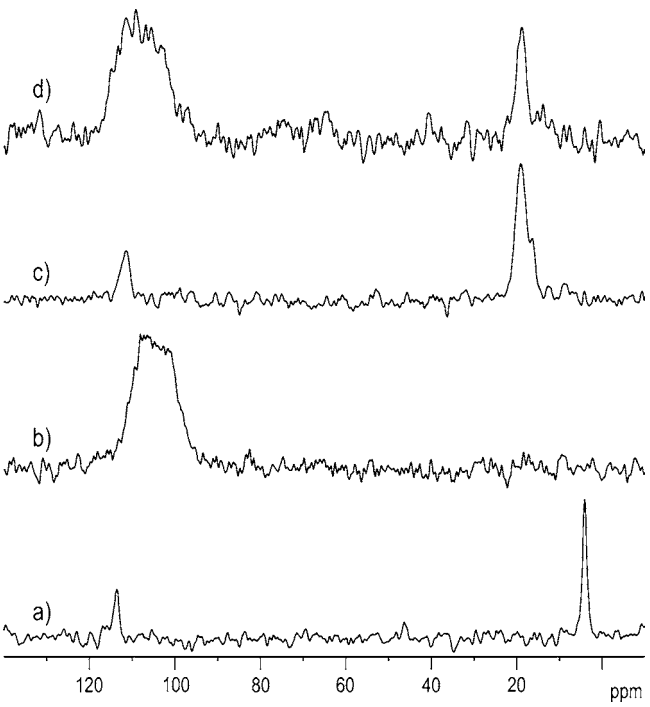

Fig. 10 ^{15}N CPMAS SS NMR spectra of (**a**) pure VIN, (**b**) PVP-CL, (**c**) Oxopocetine®, and (**d**) 1:1.1:2 coground system acquired at a spinning speed of 7 kHz.

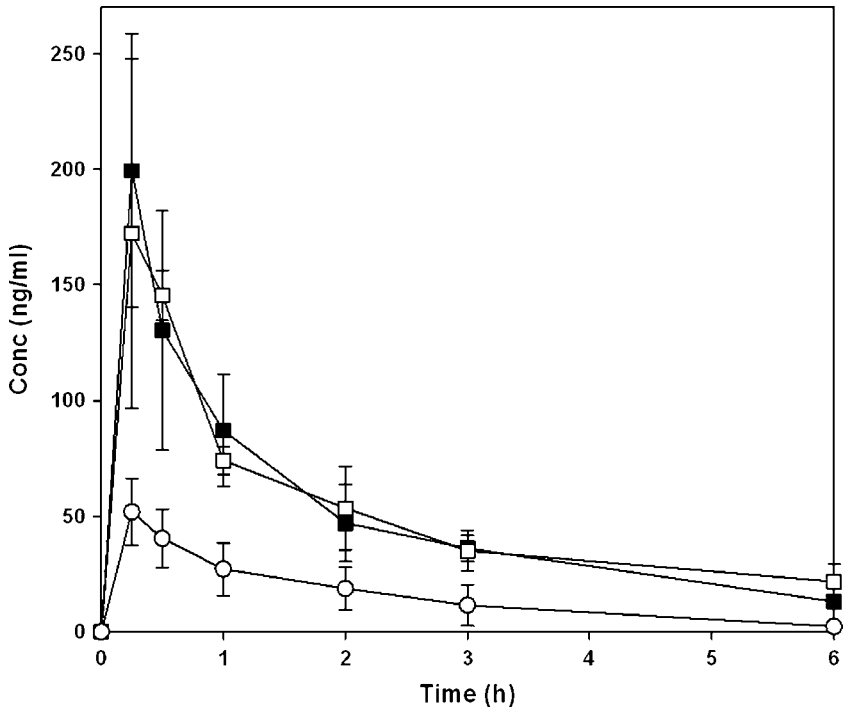

Fig. 11 Mean plasma levels (± S.D.) of VIN obtained after single dose (11 mg/kg): in 1:1.1:2 coground system (□), 1:1.1:2 PM (○) and Oxopocetine® (■).

Finally, *in vivo* tests were carried out to ascertain the increased bioavailability of VIN salt after oral administration to rats with respect its PM and to verify the bioequivalence with the commercial salt. In Fig. 11 the plasma concentration profiles are presented, whilst the pharmacokinetic parameters are listed in Table III. From these data, the great *in vivo* superiority of 1:1.1:2 coground system over its PM is clear, being four-fold more bioavailable. The bioequivalence in rats of the commercial salt and the salt prepared through mechanochemical process can be also deducted. The plasma profiles of the two salt samples are substantially super-imposable.

The solid state in the selected coground sample (1:1.1:2 wt) was monitored by repeating the DSC and XRD analyses every 9 months for a period of 18 months (for brevity, only the last sampling time was reported). These analyses testified to the stability of the amorphous state of the salt during this period of time.

The only difference on aging is the disappearing in the diffractogram (Fig. 5i) of the two signals originally at 26.3 and 32.4° of 2θ, previously attributed to free (un-reacted) citric acid. Simultaneously, in the DSC curves (Fig. 6h) a little peak appeared at about 60°C, compatible with the formation of monohydrate citric acid during storage at ambient conditions. The monohydrate is, according to literature (34), the thermodynamically stable form in the temperature range below 34°C.

CONCLUSIONS

The need to improve the VIN poor aqueous solubility to increase its oral bioavailability has been fully achieved through a solid-state mechanochemical process that has induced physical and chemical changes on the original VIN. The combination of analytical techniques, such as Raman, XPS and ^{15}N CPMAS SS NMR spectroscopies, allowed the ternary coground to be assigned as a VIN citrate in the same solid form as in the commercial salt, Oxopocetine®. The acid-base salt is obtained in absence of solvents in only 30 min of cogrinding, in presence of micronised crospovidone.

Table III VIN Pharmacokinetic Parameters After Oral Administration in Rats of the 1:1.1:2 Coground System, Corresponding PM and Oxopocetine® (Mean ± S.D., $n=4$)

Formulation	C_{max} (ng/ml)	t_{max} (h)	$AUC_{(t=6)}$ (ng h/ml)	F_{rel}
PM 1:1.1:2	51.9 ± 14.5	0.5	72.9 ± 13.1	1
1:1.1:2 Coground system	172.3 ± 75.5	0.5	309.3 ± 43.1	4.2
Oxopocetine®	199.4 ± 59.2	0.5	302.8 ± 74.9	4.2

The resulting amorphous citrate salt of VIN readily dissolves in g.i. fluids and is rapidly and highly absorbed by oral administration.

ACKNOWLEDGMENTS

The authors thank Linnea (Locarno, CH) and Covex (Madrid, ES) for kindly donating the active ingredients used in this study, D. Lenaz for his precious advices and S. Bhardwaj, from TASC-IOM-CNR AREA Science Park, Trieste, Italy, for assistance during XPS analyses.

REFERENCES

1. Bencsath P, Debrczeni L, Takács L. Effect of ethyl apovincaminate on cerebral circulation of dogs under normal conditions and in arterial hypoxia. Arzneim-Forsch/Drug Res. 1976;26:1920–3.
2. Luo Y, Chen D, Ren L, Zhao X, Qin J. Solid lipid nanoparticles for enhancing vinpocetine's oral bioavailability. J Control Release. 2006;114:53–9.
3. Csanda E, Harcos P, Bacsy Z, Berghammer R, Kenez J. Ten years of experience with Cavinton. Drug Dev Res. 1988;14:185–7.
4. Grandt R, Beitinger R, Schateltenbrand R, Braun W. Vinpocetine pharmacokinetics in elderly subjects. Arzneim-Forsch/Drug Res. 1989;39:1599–602.
5. Szakacs T, Veres Z, Vereczkey L. *In vitro-in vivo* correlation of the pharmacokinetics of vinpocetine. Pol J Pharmacol. 2001;53:623–8.
6. Kata M, Lukacs M. Enhancement of solubility of vinpocetine base with γ-cyclodextrin. Pharmazie. 1986;41:151–2.
7. Ribeiro L, Ferreira D, Veiga F. Physicochemical investigation of the effects of water-soluble polymers on vinpocetine complexationwith β-cyclodextrin and its sulfobutyl ether derivative in solution and solid state. Eur J Pharm Sci. 2003;20:253–66.
8. Ribeiro L, Falcao AC, Patricio JAB, Ferreira DC, Veiga FJB. Cyclodextrin multicomponent complexation and controlled release delivery strategies to optimize the oral bioavalaibility of vinpocetine. J Pharm Sci. 2007;96:2018–28.
9. Nie S, Fan X, Peng Y, Yang X, Wang C, Pan W. *In vitro* and *in vivo* studies on the complexes of vinpocetine with hydroxypropyl-β-cyclodextrin. Arch Pharm Res. 2007;30:991–1001.
10. Nie S, Pan W, Li X, Wu X. The effect of citric acid added to hydroxypropyl methylcellulose (HPMC) matrix tablets on the release profile of vinpocetine. Drug Dev Ind Pharm. 2004;30:627–35.
11. Miskolczi P, Vereczkey L, Szalay L, Göndöcs C. Effect of age on pharmacokinetics of Vinpocetine (Cavinton) and Apovincamininc acid. Eur J Clin Pharmacol. 1987;33:185–9.
12. Chen Y, Li G, Wu X, Chen Z, Hang J, Qin B, *et al.* Self-microemulsifying drug delivery system (SMEDDS) of vinpocetine: formulation development and *in vivo* assessment. Biol Pharm Bull. 2008;31:118–25.
13. Iosio T, Voinovich D, Grassi M, Pinto JF, Perissutti B, Zacchigna M, *et al.* Bi-layered self-emulsifying pellets prepared by co-extrusion and spheronization: influence of formulation variables and preliminary study on the *in vivo* absorption. Eur J Pharm Biopharm. 2008;69:686–97.
14. Cui SX, Nie SF, Li L, Wang CG, Pan WS, Sun JP. Preparation and evaluation of self-microemulsifying drug delivery system containing vinpocetine. Drug Dev Ind Pharm. 2009;35:603–11.
15. Hasa D, Voinovich D, Perissutti B, Bonifacio A, Grassi M, Franceschinis E, *et al.* Multidisciplinary approach on characterizing a mechanochemically activated composite of vinpocetine and crospovidone. J Pharm Sci. 2011;100:915–32.
16. Calvo F, Manresa MT. Citric acid salt of (+) vinpocetine. U.S. patent 4749707. Spain: Covex S.A.; 1988.
17. Shakhtshneider TP, Boldyrev VV. Mechanochemical synthesis and mechanical activation of drugs. In: Boldyreva E, Boldyrev V, editors. Reactivity of molecular solids. Chichester: Wiley; 1999. p. 271–311.
18. Voinovich D, Perissutti B, Grassi M, Passerini N, Bigotto A. Solid state mechanochemical activation of Silybum Marianum dry extract with betacyclodextrins: characterization and bioavailability of the coground systems. J Pharm Sci. 2009;98:4119–29.
19. Mathieu D, Nony J, Phan-Tan-Luu R. NEMRODW (New Efficient Technology for Research using Optimal Design) software. Marseille: LPRAI; 1999.
20. R Development Core Team. R: a language and environment for statistical computing. Wien: R Foundation for Statistical Computing; 2009. ISBN 3-900051-07–0. Available from: http://www.R-project.org.
21. Beleites C, Sergo V. http://hyperspec.r-forge.r-project.org for R (see reference 20); 2009.
22. Carli F, Motta A. Particle size and surface area distribution of pharmaceutical powders by microcomputerized mercury porosimetry. J Pharm Sci. 1984;73:197–203.
23. Cadelli G, Zarattini P, Stebel M. Further refinements of tail artery cannulation in conscious rats, Centro Coordinamento e Sviluppo progetti e Apparecchiature (CSPA). Settore stabulario e sperimentazione animale. Università di Trieste., FELASA-ICLAS Joint Meeting –Villa Erba, Cernobbio; 2007.
24. Vlase L, Bodiu B, Leucuta SE. Pharmacokinetics and comparative bioavailability of two vinpocetine tablet formulations in healthy volunteers by using the metabolite apovincaminic acid as pharmacokinetic parameter. Arzneim-Forsch/Drug Res. 2005;55:664–8.
25. Mura P, Faucci MT, Manderioli A, Bramanti G. Multicomponent systems of econazole with hydroxyacids and cyclodextrins. J Incl Phenom. 2001;39:131–8.
26. Lu Q, Zografi G. Properties of the citric acid at the glass transition. J Pharm Sci. 1997;86:1374–8.
27. Voinovich D, Perissutti B, Magarotto L, Ceschia D, Guiotto P, Bilia AR. Solid state mechanochemical simultaneous activation of the constituents of the silybum marianum phytocomplex with crosslinked polymers. J Pharm Sci. 2009;98:215–28.
28. Colombo I, Grassi G, Grassi M. Drug mechanochemical activation. J Pharm Sci. 2009;98:3961–86.
29. Rawlinson CF, Williams CA, Timmins P, Grimsey I. Polymer-mediated disruption of drug crystallinity. Int J Pharm. 2007;336:42–8.
30. Trapani G, Latrofa A, Franco M, Pantaleo MR, Sanna E, Massa F, *et al.* Complexation of zolpidem with 2-hydroxypropyl-β-, methyl-β-, and 2-hydroxypropyl-γ-cyclodextrin: effect on aqueous solubility, dissolution rate, and ataxic activity in rat. J Pharm Sci. 2000;89:1443–51.
31. Grassi M, Coceani N, Magarotto L, Ceschia D. Effect of milling time on release kinetics from co-grounded drug-polymer systems. Proceedings of the AAPS Annual Meeting and Exposition, October, Salt Lake City, USA; 2003.
32. Karagedov GR, Konovalova EA, Boldyrev VV, Lyachov NZ. Influence of reagent biography and reaction conditions on kinetics of lithium ferrite synthesis. Solid State Ionics. 1990;42:147–51.
33. Alonzo DE, Zhang GGZ, Zhou D, Gao Y, Taylor LS. Understanding the behaviour of amorphous pharmaceutical systems during dissolution. Pharm Res. 2010;27:608–18.
34. Groen H, Roberts KJ. Nucleation growth and pseudo-polymorphic behavior of citric acid as monitored *in situ* by Attenuated Total Reflection Fourier Transform Infrared Spectroscopy. J Phys Chem B. 2001;105:10723–30.

35. Poerwono H, Higashiyama K, Kubo H, Poernomo AT, Suharjono, Sudiana IK, *et al.* Citric acid. In: Brittain HG, editor. Analytical profiles of drug substances and excipients, vol. 28. Boston: Academic; 2001. p. 1–76.
36. Stevens JS, Byard SJ, Schroeder SLM. Salt or co-crystal? Determination of protonation state by X-Ray Photoelectron Spectroscopy (XPS). J Pharm Sci. 2010;99:4453–7.
37. Braga D, Grepioni F, Polito M, Chierotti MR, Ellena S, Gobetto R. A solid-gas route to polymorph conversion in crystalline [Fe-II (eta^5-$C_5H_4COOH)_2$]. A diffraction and solid-state NMR study. Organometallics. 2006;25:4627–33.
38. Chierotti MR, Gobetto R. Solid-state NMR studies of weak interactions in supramolecular systems. Chem Commun. 2008;14:1621–34.